Spring 2022

Predicting radiated emissions from a cable harness through component level tests

Fuwei Ma

Department:

PREDICTING RADIATED EMISSIONS FROM A CABLE HARNESS THROUGH COMPONENT LEVEL TESTS

by

FUWEI MA

A THESIS

Presented to the Graduate Faculty of the

MISSOURI UNIVERSITY OF SCIENCE AND TECHNOLOGY

In Partial Fulfillment of the Requirements for the Degree

MASTER OF SCIENCE

in

ELECTRICAL ENGINEERING

2022

Approved by:

Dr. Daryl G. Beetner, Advisor
Dr. Chulsoon Hwang
Dr. DongHyun Kim

PUBLICATION THESIS OPTION

This thesis consists of the following paper formatted in the style used by the Missouri University of Science and Technology.

Paper I: Pages 2-35 are intended for submission to 2022 IEEE International Symposium on Electromagnetic Compatibility, Signal & Power Integrity.

ABSTRACT

In this work, a procedure is developed to predict the radiated emissions from a cable harness using component-level tests. Direct measurement on the engine control unit is utilized to accurately characterize the equivalent common mode source voltages and impedance associated with the device. The cable harness geometry is reduced using the equivalent cable bundle approach by lumping wires according to the source and load impedance compared with characteristic impedance of the harness, which dramatically reduces the measurement effort and allows practical 3D full-wave simulation of the radiated emissions. Radiated emissions are predicted from an engine control unit (ECU) and an attached harness under a variety of harness configurations. The proposed procedure was validated through the comparisons of radiated emissions and measurements. Simulated emissions matched those from measurements within 6 dB across multiple cable configurations.

ACKNOWLEDGMENTS

This thesis is based upon work supported partially by the National Science Foundation under Grant No. IIP-1916535.

First, I would like to show my deep gratitude to my advisor, Dr. Beetner, and then thank all the member from EMC Laboratory to help me achieve one of most important steps in my life.

Second, sincere thanks are shown to my parents for believing me, and unreservedly supporting me to explore the wider world.

In addition, the most important thing is that I want to show my special gratitude to Miss. Bo Wen, who is one of the most beautiful and kind girl during the first twenty years of my life, for her understanding and great trust to me, and she always listens to my stories and complaints with great empathy and patience like the elder sister treating her innocent younger brother, smiling gently, but guiding me silently and powerfully, giving me unparalleled spiritual support to struggle with and survive from those dark times, making me sincerely look forward to the future stories with her in the next several decades years. I believe that she is my moonlight, shining brightly and softly in those painful nights, slowly soothing my pains and sorrows. The hard times we experienced together have become the nourishment for our great love to grow and be prosperous, and will inject the warmth and hope into the future to face difficulties fearlessly.

Finally, at this moment, any further extra word is redundant, and I just want to appreciate all the people who have had given me help, again.

TABLE OF CONTENTS

Page

LIST OF ILLUSTRATIONS

Figure Page

PAPER I

SECTION

1. INTRODUCTION

The ability to predict system-level radiated emissions early in the design process is critical to the design of complex modern vehicles. After the system has been assembled, fixing the radiated emissions problem will be hard, expensive and time-consuming. Usually, the solutions may cause negative impact on the design constraints of products, such as the size, shape and prime cost. However, predicting the system-level radiated emissions is challenging, because the substantial information about the system would be required to perform the simulations. Individual components of course will be tested before they are integrated with the system level. Passing tests at component level is rarely sufficient to guarantee the radiated emission passing the tests at system level, due to the fact that some tiny differences between the harness configurations in component-level test and system-level test may dramatically influence on the common mode current along the harness and thus the radiated emissions from the harness. Hence, there is a demand to the method allowing accurate prediction of system-level radiated emissions in the early design process with some simple component-level tests.

The following part proposes a method to experimentally characterize the common mode source information and thus predict system-level radiated emissions using a relatively small number of component-level measurements. The number of measurements and complexity of simulations are reduced significantly by characterizing only a few equivalent sources for the electronic component, based on the size of the expected source and load impedance driven by the component [1]. These equivalent sources are characterized using a special designed fixture board standing on a vertical plane along the harness, and then the equivalent common mode source is used to drive a simplified harness model derived from a full-wave simulation to predict radiated emissions. Comparison results of measured and predicted radiated emissions demonstrate the potential of the approach.

PAPER

I. PREDICTING RADIATED EMISSIONS FROM A CABLE HARNESS THROUGH COMPONENT LEVEL TESTS

FUWEI MA
Department of Electrical & Computer Engineeringg
Missouri University of Science and Technology
Rolla, Missouri 65409–0050
Tel: 573–341–6622, Fax: 573–341–4115
Email: mafu@mst.edu

ABSTRACT

In automotive and agricultural systems, an electronic component connected to a harness is a common source of radiated emissions. Predicting system-level radiated emission early in the design process is essential to allow radiated emissions problems to be fixed easily and at a low cost. In this work, a method is proposed for characterizing common mode sources from a component that can drive a wiring harness, and for predicting the resulting radiated emissions from the harness. To reduce the number of measurements, harness wires connected to similar load impedance are grouped together to construct a simplified and equivalent harness model. This procedure utilizes several simple measurements to characterize the source information inside the engine control unit. Radiated emissions are then predicted through a combination of circuit simulation and 3D simulation with ADS and CST. The proposed procedure was validated through the comparisons of radiated emissions and measurements. Simulated emissions matched those from measurements within 6 dB across multiple cable configurations.

Keywords: Engine Control Unit, Cable Harness, Harness Reduction, Radiated Emissions, Equivalent Source, System-level, Prediction, Electromagnetic Compatibility.

1. INTRODUCTION

In automotive systems, the engine control unit (ECU) connected to a harness is a common source of radiated emissions. The common-mode current on harness is often strong responsible for system level radiated emissions (RE). Solving system-level radiated emission problems is expensive and time-consuming and can impact the quality of the design, such as its size and weight [1], [2]. Predicting radiated emissions performance early in the design process is critical to easily and inexpensively solve emissions issues. Component level tests alone, however, are rarely sufficient because passing component-level tests does not guarantee the system level could also pass radiated emissions requirements. It is not unusual to see a substantial difference between common mode currents and radiated emissions observed in component-level and system-level tests [3].

An approach is proposed in [4] to predict vehicle level radiated emissions using conducted emissions from the module and harness radiation efficiencies. In this approach, a transfer function is measured for the current on a given cable to the voltage at a receiving antenna, and then the overall radiated emission is predicted from a measurement of the component level current. However, it is often impractical because of the modern engine control unit (ECU) in a real vehicle usually driving hundreds of wires.

[5] developed a three-dimensional (3D) PEEC method to predict the radiated fields from automotive cables. The PEEC method is observed to be computationally efficient, but it is not capable of dealing with multi-wire cable harnesses. A reduction method of multi-wire cable harnesses is proposed [6], by grouping the wires according to their source and load impedance compared with the characteristic impedance of harness. With the reduced equivalent conductors, the 3D full-wave simulation for the cable harness model becomes computationally feasible. The authors in [7] utilized 3D full-wave simulation to predict the susceptibility of the cable harness, which can be treated as the reciprocal of the radiated emission problem. The equivalent source voltages were not required in [6] and [7] since they were exploring susceptibility to known sources.

In [8], a segmentation approach was used to model radiated emissions from test setup using commercially available EM simulation tools to characterize the cable harness, along with full information about the sources driving the harness. The method proposed in [2] acquires equivalent source impedance and source voltages by solving non-linear equations, which introduces error and increases the solving time. A method is proposed in [9] to obtain the equivalent source voltages and impedances through direct measurement. The predicted common-mode current matched well with the measured results, which validated the equivalent source information.

In this work, a procedure is developed to predict the radiated emissions from a cable harness using component-level tests. The novelty of this procedure is developing a universal source characterization method by direct measurements to accurately extract equivalent source voltages and source impedances from ECUs with different shapes, and then successfully predicting the peak levels of radiated emissions within 6 dB only based on component level tests. The cable harness geometry is reduced using the equivalent cable bundle approach in [6], which dramatically reduces the measurement effort and allows practical 3D full-wave simulation of the radiated emissions. Comparison of measured and predicted radiated emissions demonstrate the potential of this approach.

This paper is organized as follows: Section 2 explains the breakdown of system-level measurement setup, and shows the different parts needing to be modeled in this proposed procedure. Section 3 characterizes the sources information and builds the equivalent model of common mode source. Section 4 describes the model of common-mode loads. Section 5 summarizes the method used to develop an equivalent harness model and depicts the geometry reduction of the cable harness. Section 6 shows the antenna model. Section 7 assembles the characterized modules into a prediction model for the radiated emissions. Finally Section 8 discusses the measurement validation results, the limitation of the proposed procedure, and its future development.

2. THE SYSTEM-LEVEL MEASUREMENT SETUP

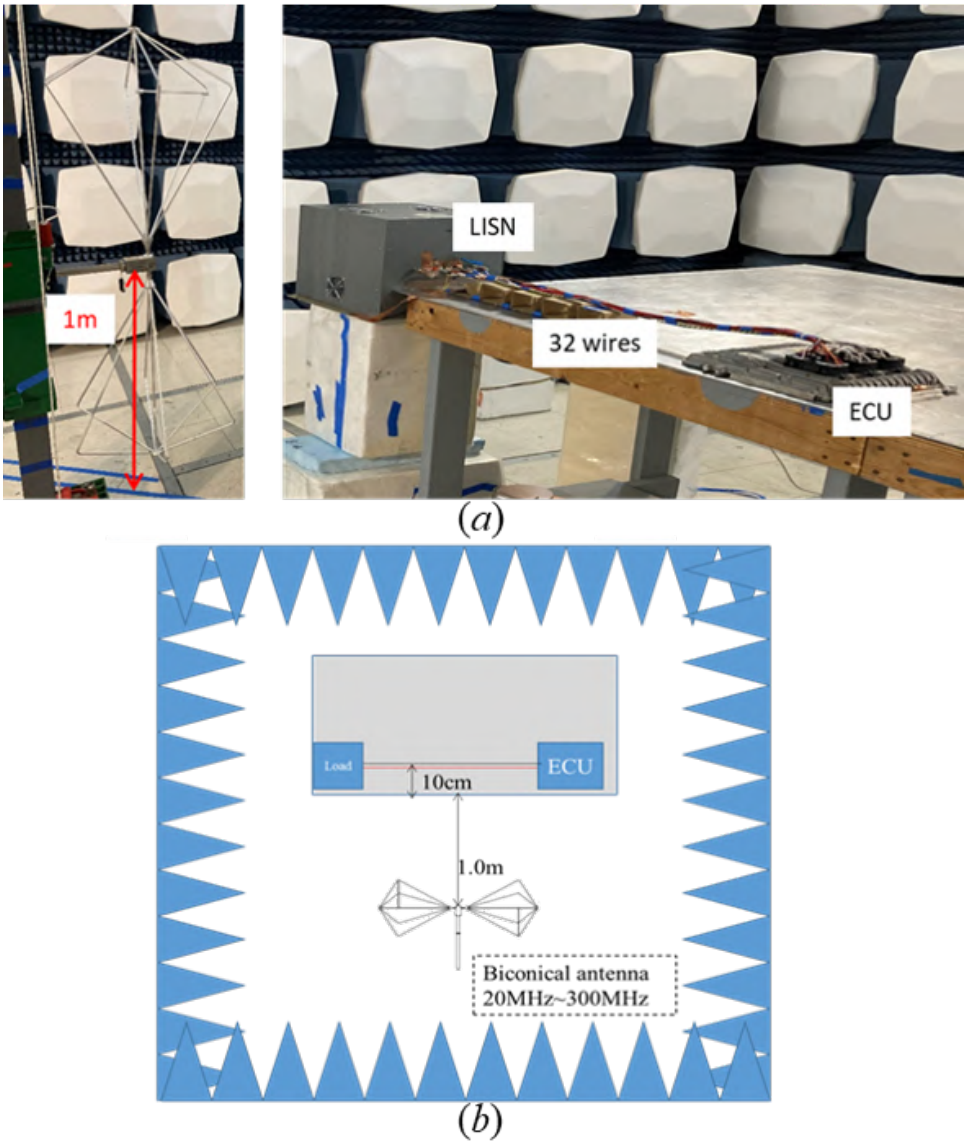

Figure 1. Setup of a simplified version of system-level radiated emission test. (a) The receiving antenna (1m above the floor), the ECU, cable harness, and loads. (b) Top view of the test setup.

The test setup in Figure 1 displays a simplified version of the system-level radiated emission test. The key components of an actual system-level test setup are still present: the noise source, the cable harness, and reflectors. This test setup is decomposed into

several modules: ECU, Loads (LISN and other loads), Harness, Antenna, as shown in in Figure 2. These modules can be characterized separately and simultaneously, which boosts the prediction procedure.

The cable harness contains 32 wires that are connected to 32 pins on the ECU end. There are 14 power wires in this harness. Among the power wires, 6 wires are connected to 12 V, and other 8 wires connected to 0 V reference. The other extremity of these 14 power wires are connected to the LISN (FCC-LISN-50-25-2), then the DC supply. Other 18 wires are connected to designed PCB loads. Therefore, the loading impedances of these wires are known. All wires are run in the same branchless harness, which is about 1m long. The harness is grouped into four groups, according to the similar loads (details in Section 5).

The receiver side of this setup contains the biconical antenna, a low noise amplifier, and the spectrum analyzer. A model of the antenna can be built in 3D full-wave simulation environment, along with the ECU and cable harness. Such simulation model requires accurate reproduction of the antenna properties, namely, antenna factor, gain, etc. Besides, this model will be hardly computable if a complex harness is present. Section 5 describes how the cable harness geometry is reduced, and Section 6 describes the modeling of the biconical antenna. In the full-wave simulation model, the LISN and ECU will be just metal box.

3. MODEL FOR THE COMMON-MODE SOURCE

[2] proposed an indirect method of measuring common-mode currents with the variety of harness length to characterize the equivalent sources information inside the ECU by grouping wires of the harness bundle into two groups; however, this method made many simplified assumptions about the system, and at the same time, it was susceptible to interference from measurement errors, so there was very strict requirements for measurement accuracy of common-mode currents. In this paper, the source information are directly measured with a special designed fixture of a vertical board, as shown in Figure 2.1.

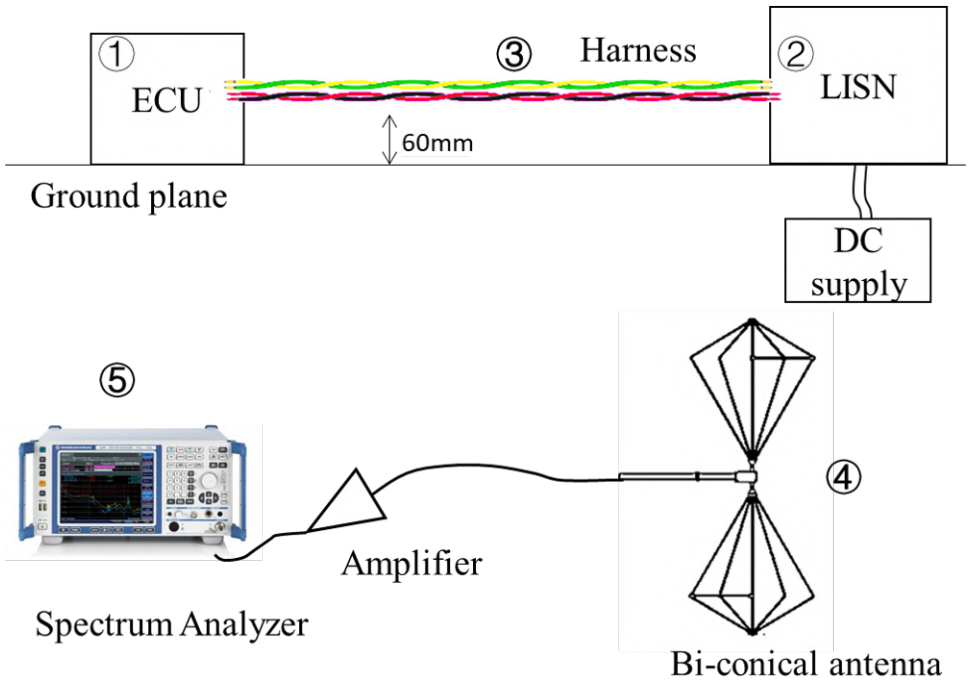

Figure 2. Block diagram of the system-level setup. The setup is divided into 5 parts, each part is characterized separately.

Considering the shape of ECU, the ECU1, 2, and ECU3 are separated by the metal, and the height of this ridge is about 1.2 cm, shown in Figure 4. To characterize the source information inside the ECU, one way is to build a horizontal board on the top to connect the pins together corresponding to grouped wires and then the equivalent sources could be measured, but for this horizontal board, the height between pins and horizontal board will introduce large parasitic inductance and capacitance. Finding a vertical plane on the harness to measure the source can help to reduce the parasitics and hence a vertical source board is designed to characterize equivalent four-port source information rather than horizontal board.

As Figure 2.1 shown, a DC block is added between the pin of 12V wires and pin of GND wires on the surface of the vertical source board to prevent shorting at DC. The reference plane of the board is electrical connected with the chassis of ECU to minimize

(*a*)

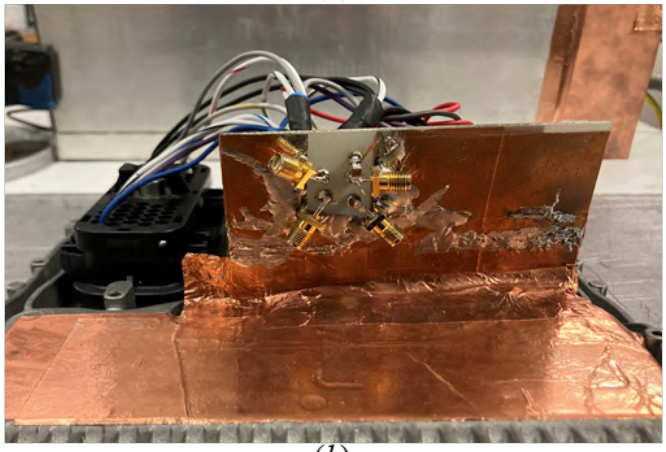

(*b*)

Figure 3. ECU and characterization board. (a) Top view of fixture. (b) Front view of fixture and four SMA ports.

parasitic inductance in the measurement. On the source board, the SMA connector is soldered for each group, from which the coaxial cables can be connected to a spectrum analyzer or an oscilloscope to characterize the source information in frequency domain or time domain.

The equivalent circuit for sources is shown in Figure 5. The pivotal part is a Y4p file describing this four-port source admittance network. The pins and wires belonging to group 1, group 2, group 3 and group 4 are lumped together on the source board to connect with the corresponding SMA port 1, 2, 3 and port 4, respectively. The current sources I1, I2,

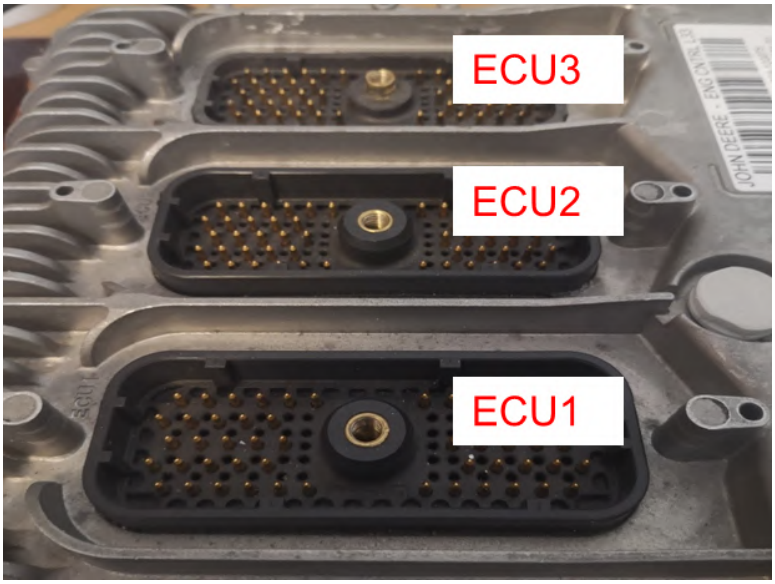

Figure 4. Shape of ECUs.

I3 and I4 are the equivalent parallel current source for each group after the transformation procedure. They are based on the source voltages measured at the four ports on source board.

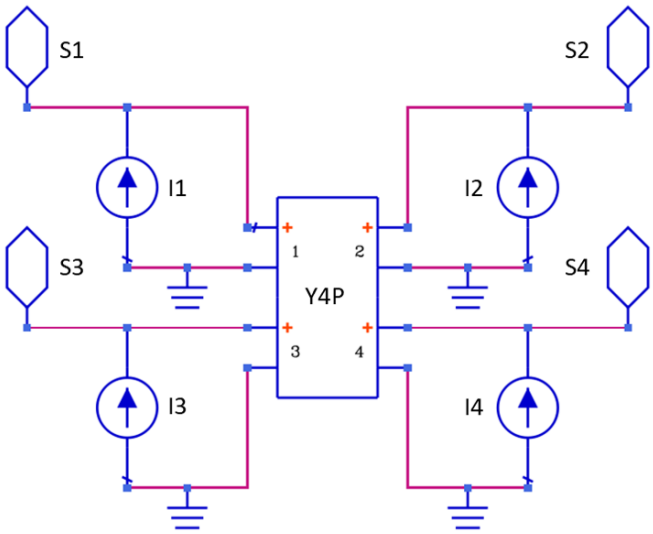

Figure 5. Equivalent source circuit in ADS.

3.1. FOUR-PORT SOURCE IMPEDANCE NETWORK CHARACTERIZATION

Source impedance network could be measured by this measurement setup in Figure 6. A vector network analyzer (VNA) with only two ports (Agilent E5071c) were used for characterization. Due to the limit number of ports, two-port measurement was finished at single time while other two ports were terminated with 50 Ω loads. A s2p file recording the S-parameters could be obtained for each measurement. Six s2p files of each pair of ports needed combining to get one s4p file and after converting the measured S-parameters to Y-parameters, the Y4p file describing four-port source admittance network was obtained.

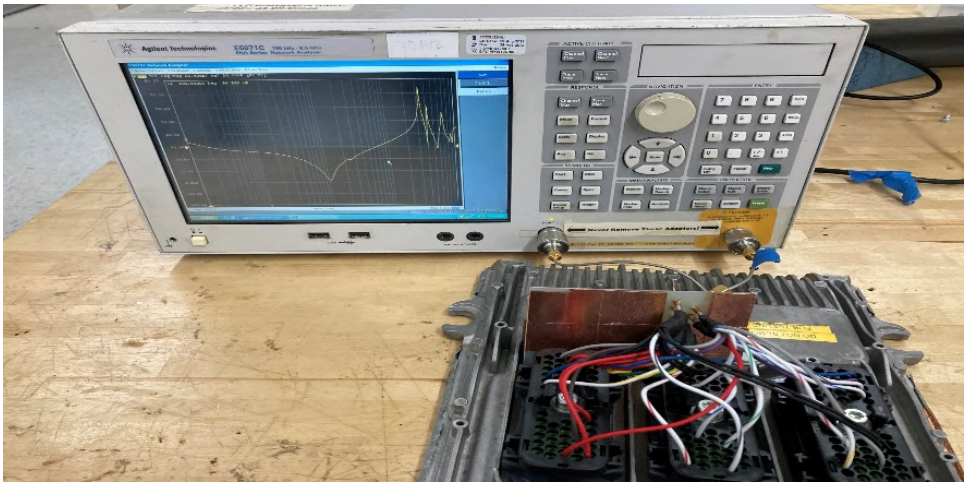

Figure 6. Setup for the impedance measurement.

3.2. FOUR-PORT SOURCE MAGNITUDE MEASUREMENT

The setup with a spectrum analyzer (SA) used to measure the four-port source magnitude is shown in Figure 7. The spectrum analyzer was connected to one port with other three ports terminated with 50 Ω loads while the ECU was running and powered by a 12V battery. The source magnitude of one group is measured at single time and finally the source magnitudes of four equivalent groups could be measured at each SMA port.

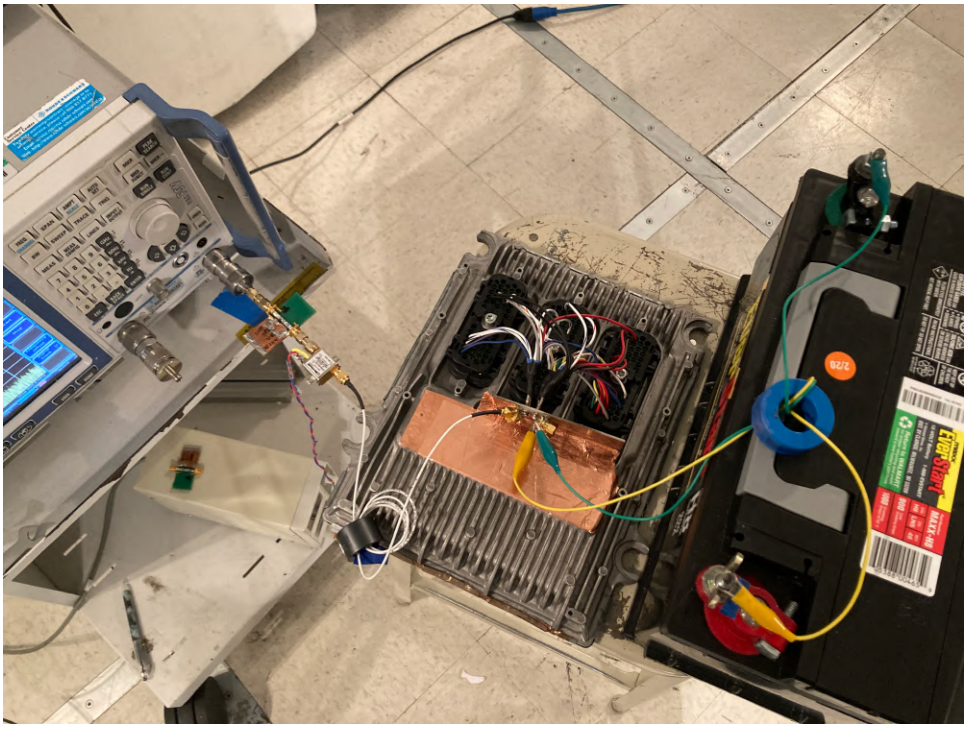

Figure 7. Setup for source magnitude measurement.

Due to the requirements of system-level EMI test, the same conditions were required for source magnitude measurement. The resolution bandwidth (RBW) was set as 100kHz and Max-hold was required for SA detection mode. The ferrite must be added on SA input port to suppress the common-mode noise.

3.3. TIME DOMAIN SOURCE VOLTAGE MEASUREMENT

The setup shown in Figure 8 wwas used for source voltage measurement in time domain to characterize the phase information of the sources. An oscilloscope was connected to four ports with the ECU activated by the same 12V battery. The four channels of the oscilloscope were triggered at the same time with the group 1 which contained Vcc and Vdd wires set as trigger source. The time domain waveforms with 2 ms duration time and 2GSa/s sampling rate of four channels were recorded.

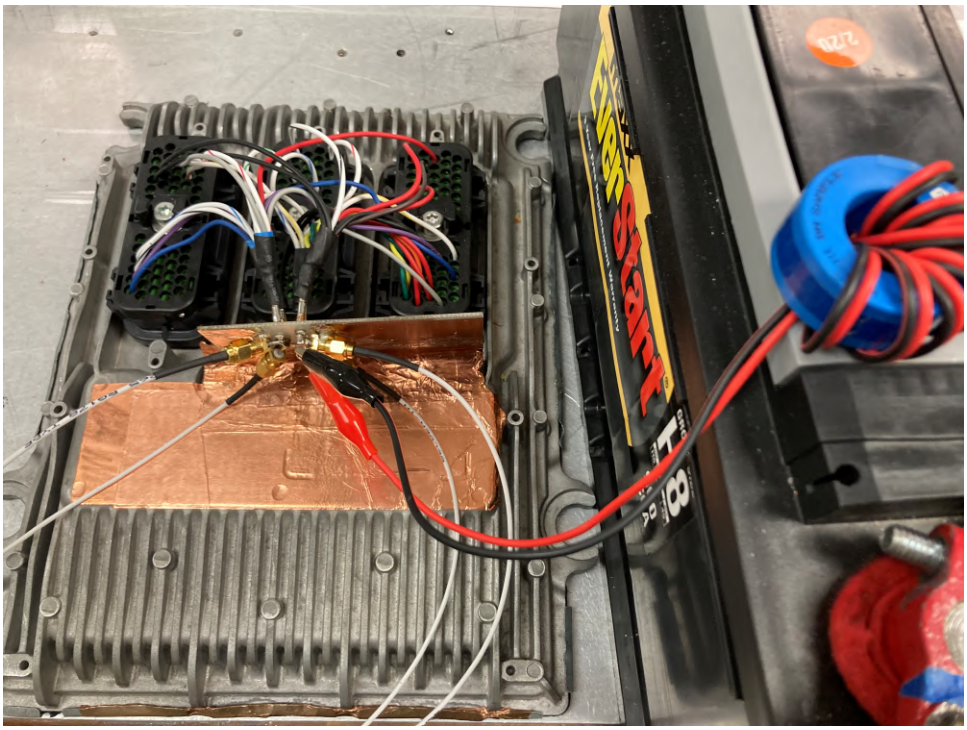

Figure 8. Setup for time domain source voltage measurement.

Because of the 100 kHz RBW requirement of EMI test, the measured time sequence also needs to be transformed in frequency domain with 100 kHz RBW. The waveforms could be cut into hundreds or thousands of fragments of 10 μs duration time with a slide window. For each window, the short-time Fourier Transform (STFT) was executed. The relative phase between the source voltages of each group must be characterized to predict the common mode current, since the common-mode current is a sum of the currents along each equivalent conductor in the harness. The phase difference between two sources is defined as $\Delta\theta_{21} = phase(V_2) - phase(V_1)$, where V_1 and V_2 are the spectrums of measured voltage sources of group 1 and group 2. Similarly, $\Delta\theta_{31} = phase(V_3) - phase(V_1)$, and $\Delta\theta_{41} = phase(V_4) - phase(V_1)$ also need to be determined.

Figure 9 shows the phase difference between voltage sources of group 1 and group 2 for one thousand 10-μs windows. The short-time Fourier Transform results are plotted in a surface map. The x-axis is the number of the short-time window, while the y-axis is the

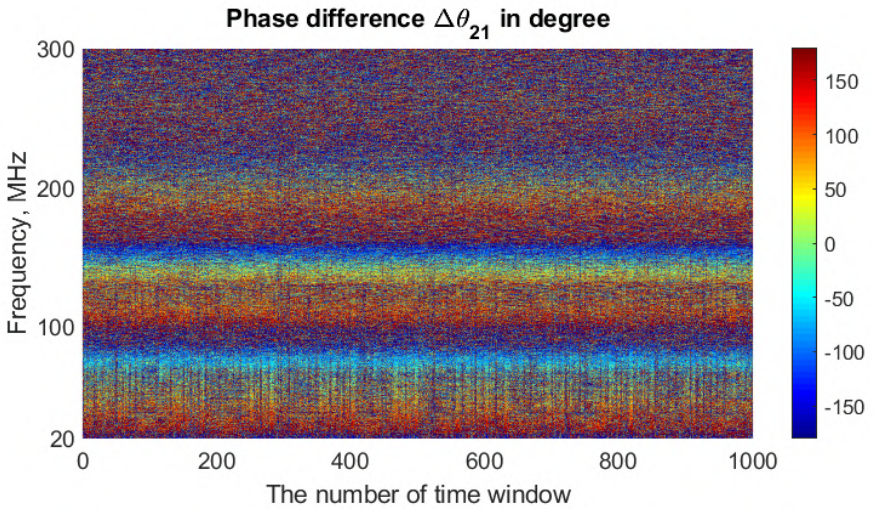

Figure 9. Phase difference between the V_2, V_1 over all 1000 time-windows, over frequencies from 20-300 MHz.

frequency from 20-300 MHz. The consistency in color across the windows indicates a strong relationship of phase informationthe between two measured voltages. The Figure 10 plots the distribution of phase difference for one thousand 10-μs windows at a single frequency (i.e., 75 MHz). The results prove that the probability distribution of phase difference obeys the Gaussian normal distribution.

According to this prior knowledge, the phase value with maximum likelihood across all measurements could be the result of statistical estimation to predict radiated emissions. Above 200 MHz, the signals are weak, and it is difficult to find a useful maximum likelihood estimate. This limitation has little impact on predicted results, since the radiated emission above 200 MHz is lower than the instrument noise floor.

Source magnitude can be also calculated by the time domain measurement data with the oscilloscope, however, the frequency domain measurement with the spectrum analyzer is necessary to obtain more precise signal with better characterized features from the source, especially in some frequency range the signal magnitude even lower than the noise floor of the oscilloscope.

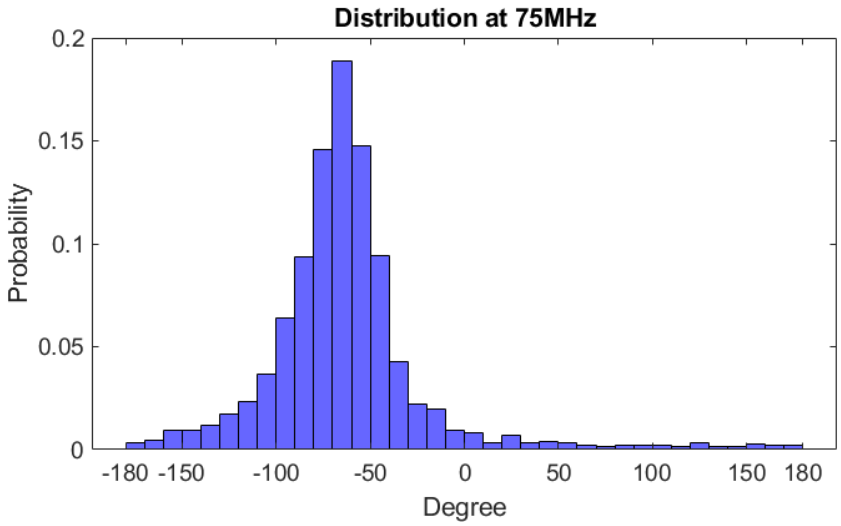

Figure 10. Distribution of phase difference at 75 MHz.

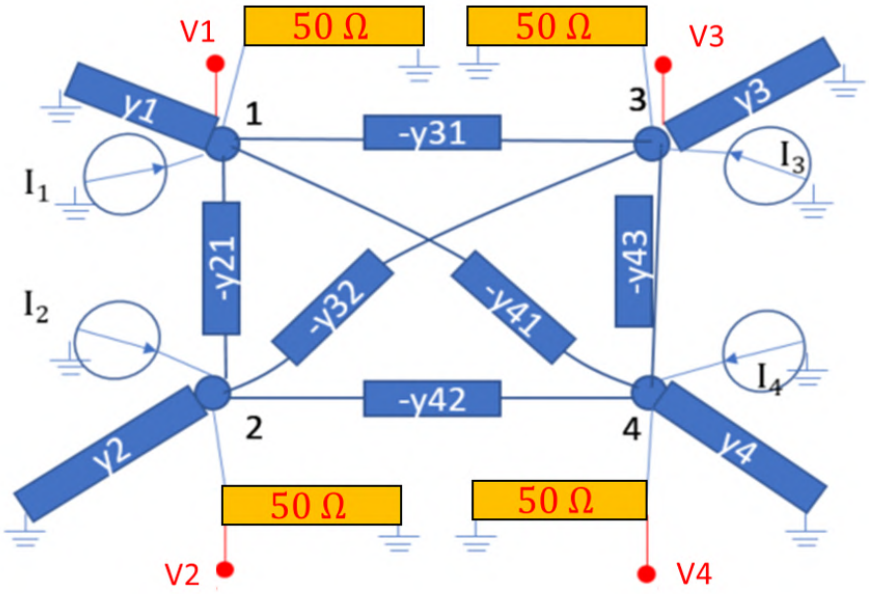

Figure 11. Admittance network and current sources.

The equivalent 4-port admittance network and current sources are shown in Figure 11. The V_1, V_2, V_3 and V_4 are the measured source voltages at the four different SMA ports of each group on source board, and these source voltage results are measured on 50

Ω system. So far, the measured complex voltages are obtained. The equivalent parallel current sources could be derived by a straightforward transformation. The Figure 12 plots the current flows.

According to the admittance network and current flows, the following relationships can be determined easily:

$$\begin{aligned} Y_1 &= Y_{11} + Y_{12} + Y_{13} + Y_{14} + 0.02, \\ Y_2 &= Y_{22} + Y_{21} + Y_{23} + Y_{24} + 0.02, \\ Y_3 &= Y_{33} + Y_{31} + Y_{32} + Y_{34} + 0.02, \\ Y_4 &= Y_{44} + Y_{41} + Y_{42} + Y_{43} + 0.02. \end{aligned} \tag{1}$$

For current relation:

$$\begin{aligned} & i_{11} = V_1 Y_1, i_{22} = V_2 Y_2, \\ & i_{33} = V_3 Y_3, i_{44} = V_4 Y_4, \\ & i_{12} = (V_2 - V_1) Y_{12}, i_{13} = (V_3 - V_1) Y_{13}, \\ & i_{14} = (V_4 - V_1) Y_{14}, i_{23} = (V_3 - V_2) Y_{23}, \\ & i_{24} = (V_4 - V_2) Y_{24}, i_{34} = (V_4 - V_3) Y_{34}. \end{aligned} \tag{2}$$

For current sources I1, I2, I3 and I4 are given:

$$\begin{aligned} I_1 &= i_{11} + i_{12} + i_{13} + i_{14}, \\ I_2 &= -i_{12} + i_{22} + i_{23} + i_{24}, \\ I_3 &= -i_{13} - i_{23} + i_{33} + i_{34}, \\ I_4 &= -i_{14} - i_{24} - i_{34} + i_{44}. \end{aligned} \tag{3}$$

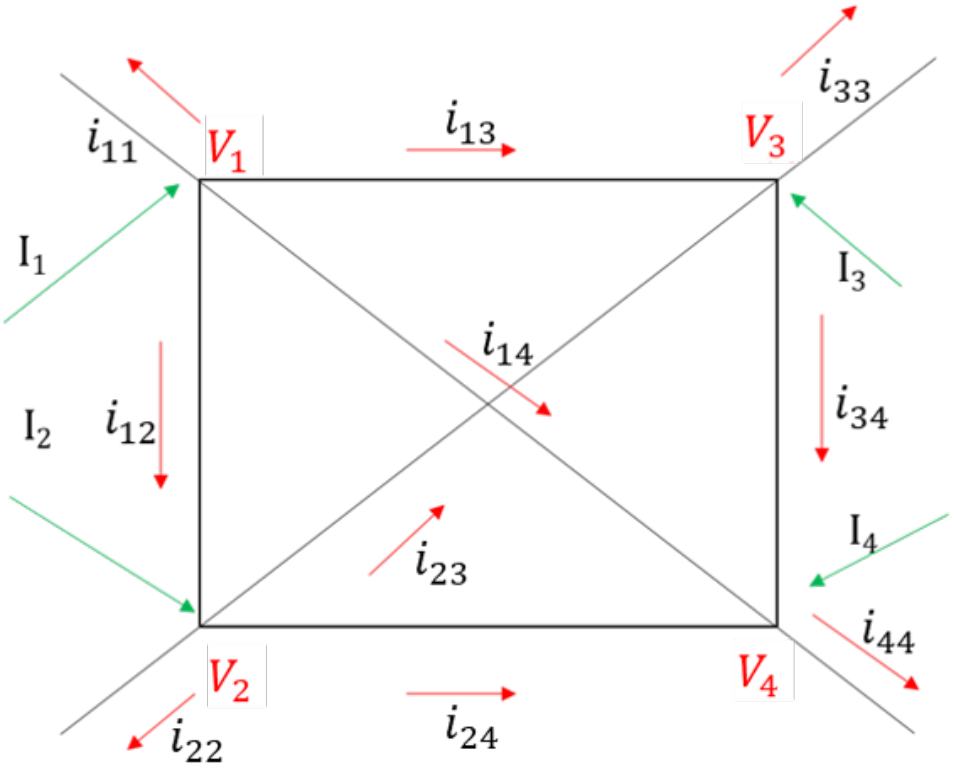

Figure 12. Current flows.

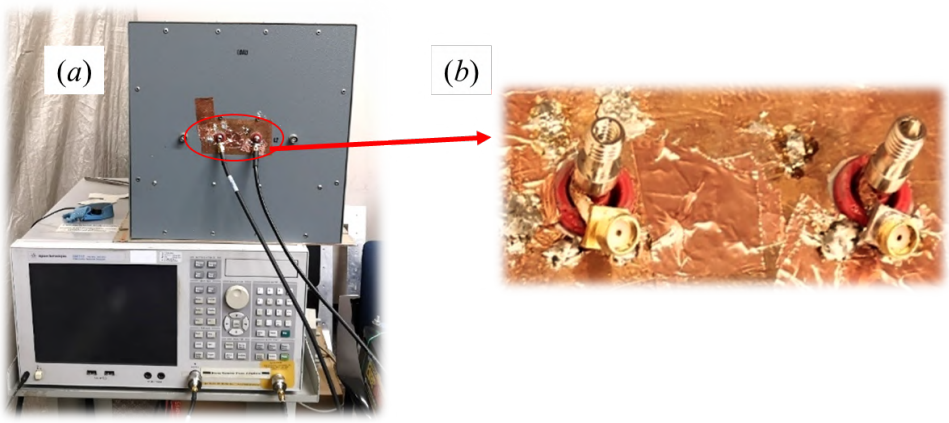

Figure 13. (a) The LISN characterization setup (b) The test fixture for LISN characterization.

4. MODEL FOR THE COMMON-MODE LOAD

Harness reduction assumes similar sources and loads within the same group,hence the identical current distribution along the wires belonging to one group, which allows loads to be approximated as “shorted” together.

For the LISN part, the LISN was measured using a 2-port VNA. Test ports were soldered to the LISN, as shown Figure 13. The measured impedance is shown in Figure 14. As expected, the input impedance below 100 MHz is approximately 50 Ω, as specified for this device.

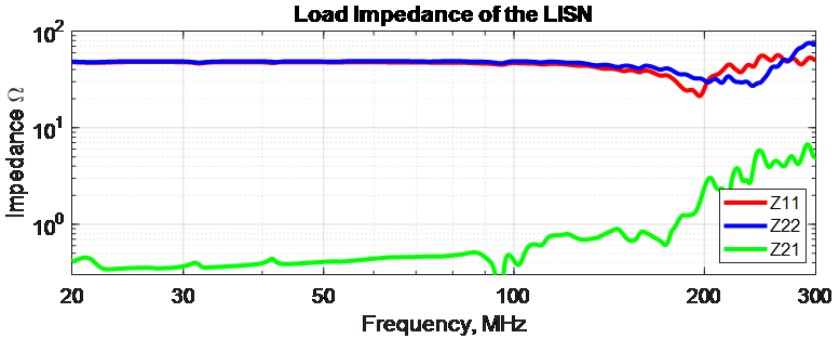

Figure 14. The measured impedance of the LISN.

For other three groups, for example, the loads of the wires belonging to group 2 are all high resistive loads (shown in Figure 15), and the current along each wire is assumed identical, so they can be treated as connecting to the same single node, which is shown in Figure 16.

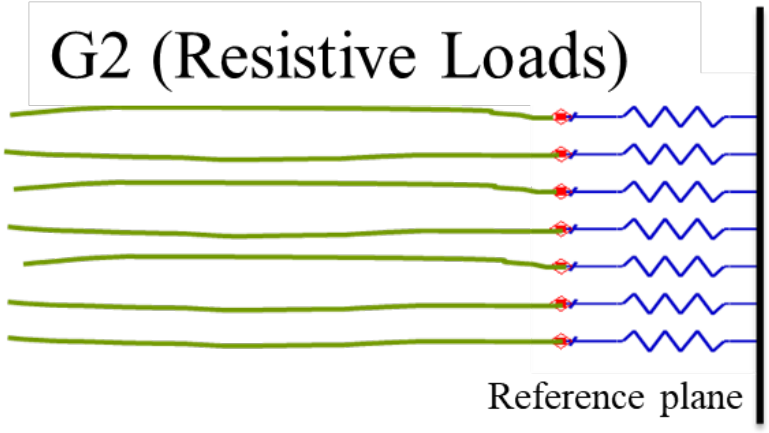

Figure 15. Resistive loads of group2.

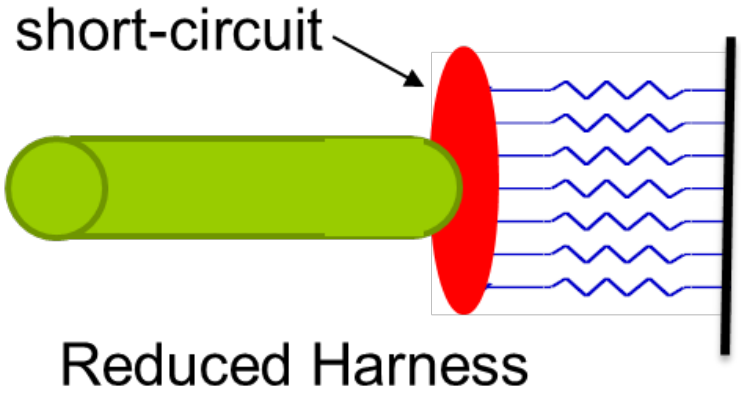

Figure 16. Equivalent common-mode load of group2.

5. REDUCTION MODEL FOR THE CABLE HARNESS

The cable harness has a significant influence on radiated emission [4][10]. Though the complete harness models with every single conductor can be built and solved by full-wave modelling, these models would be hard to build with up to one hundred sing-ended wires and computationally expensive to simulate and solve, especially modelling the radiated emissions from realistic setups for CISPR 25. With conductors of the harness grouped into equivalent bundles which can be simplified as a single wire [6], the complexity of the harness will be reduced dramaticallly.

The Wires are lumped together according to the features of their source and load impedance, and the equivalent conductor has the specific cross-section geometry so that it maintains the correct equivalent characteristic impedance [7]. Hence, the equivalent multiconductor transmission line is able to maintain the most important qualities of the original harness for the prediction of radiated emissions. The harness is divided into groups based on the wires with similar load impedance and compared with the characteristic

impedance of the wire transmission line (i.e., loads impedance are all high resistive or inductive, and both much greater or less than the the characteristic impedance) to start the harness reduction procedure.

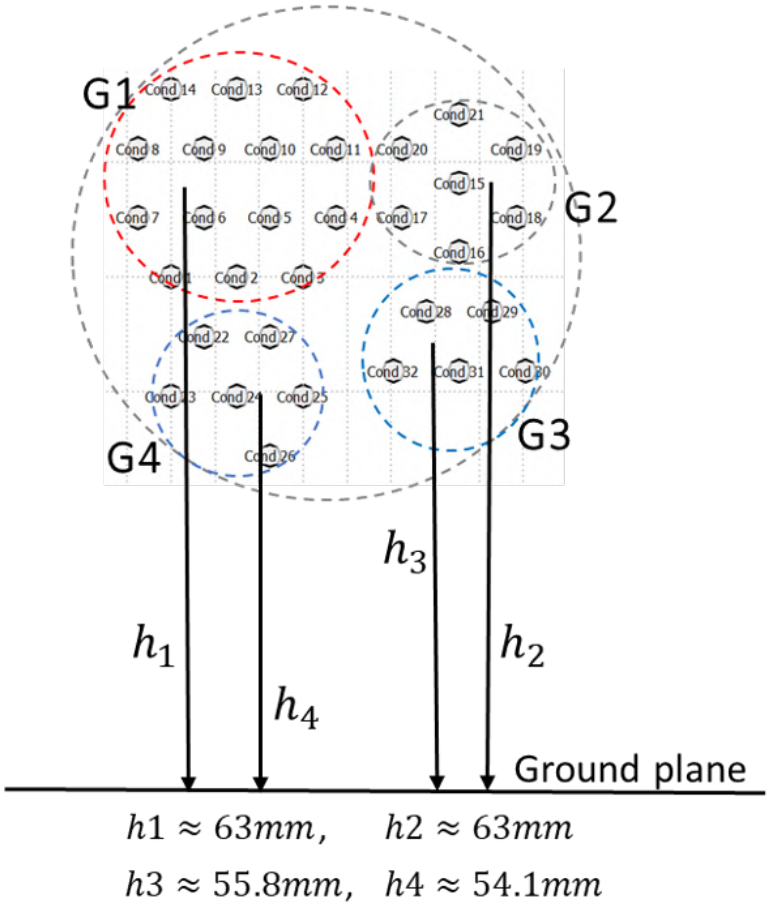

Figure 17. The approximated cross-section of the cable harness.

The 32 wires in the harness studied here were divided into four groups: the first group (which will be called group G1) for the fourteen power wires (12V and 0V) which are connected to the LISN, the second group (G2) contained 7 wires with all high resistive loads greater than thousands Ω, the third group (G3) with 5 wires connected to inductive loads around 120 nH, and the last group (G4) included some wires with small capacitance. As a result, the 32-wire cable harness was reduced to an equivalent 4-wire multiconductor transmission line for modelling and measurement purpose.

Ignoring the translational variations in the harness for simplicity, the 32-wire harness can be described using per unit length RLGC matrices. The R and G terms represent the wire conductor and dielectric loss terms, respectively. These two terms are both negligible for frequency range below 300 MHz. The L and C matrices can be determined by the cross-section geometry of the original 32-wire harness (shown in Figure 16). If the L and C matrices of original harness are given by,

$$\bar{\bar{L}} = \begin{bmatrix} L_{1,1} & \dots & L_{1,32} \\ \dots & \dots & \dots \\ L_{32,1} & \dots & L_{32,32} \end{bmatrix}, \bar{\bar{C}} = \begin{bmatrix} C_{1,1} & \dots & C_{1,32} \\ \dots & \dots & \dots \\ C_{32,1} & \dots & C_{32,32} \end{bmatrix} \tag{4}$$

then the equivalent 4-wire harness will be given by [7]:

$$\bar{\bar{L}}_{reduced} = \begin{bmatrix} \frac{\sum_{i=1}^{14}\sum_{j=1}^{14} L_{ij}}{N_1 N_1} & \frac{\sum_{i=1}^{14}\sum_{j=15}^{21} L_{ij}}{N_1 N_2} & \frac{\sum_{i=1}^{14}\sum_{j=22}^{26} L_{ij}}{N_1 N_3} & \frac{\sum_{i=1}^{14}\sum_{j=27}^{32} L_{ij}}{N_1 N_4} \\ \frac{\sum_{i=15}^{21}\sum_{j=1}^{14} L_{ij}}{N_2 N_1} & \frac{\sum_{i=15}^{21}\sum_{j=15}^{21} L_{ij}}{N_2 N_2} & \frac{\sum_{i=15}^{21}\sum_{j=22}^{26} L_{ij}}{N_2 N_3} & \frac{\sum_{i=15}^{21}\sum_{j=27}^{32} L_{ij}}{N_2 N_4} \\ \frac{\sum_{i=22}^{26}\sum_{j=1}^{14} L_{ij}}{N_3 N_1} & \frac{\sum_{i=22}^{26}\sum_{j=15}^{21} L_{ij}}{N_3 N_2} & \frac{\sum_{i=22}^{26}\sum_{j=22}^{26} L_{ij}}{N_3 N_3} & \frac{\sum_{i=22}^{26}\sum_{j=27}^{32} L_{ij}}{N_3 N_4} \\ \frac{\sum_{i=27}^{32}\sum_{j=1}^{14} L_{ij}}{N_4 N_1} & \frac{\sum_{i=27}^{32}\sum_{j=15}^{21} L_{ij}}{N_4 N_2} & \frac{\sum_{i=27}^{32}\sum_{j=22}^{26} L_{ij}}{N_4 N_3} & \frac{\sum_{i=27}^{32}\sum_{j=27}^{32} L_{ij}}{N_4 N_4} \end{bmatrix}, \tag{5}$$

$$\bar{\bar{C}}_{reduced} = \begin{bmatrix} \sum_{i=1}^{14}\sum_{j=1}^{14} C_{ij} & \sum_{i=1}^{14}\sum_{j=15}^{21} C_{ij} & \sum_{i=1}^{14}\sum_{j=22}^{26} C_{ij} & \sum_{i=1}^{14}\sum_{j=27}^{32} C_{ij} \\ \sum_{i=15}^{21}\sum_{j=1}^{14} C_{ij} & \sum_{i=15}^{21}\sum_{j=15}^{21} C_{ij} & \sum_{i=15}^{21}\sum_{j=22}^{26} C_{ij} & \sum_{i=15}^{21}\sum_{j=27}^{32} C_{ij} \\ \sum_{i=22}^{26}\sum_{j=1}^{14} C_{ij} & \sum_{i=22}^{26}\sum_{j=15}^{21} C_{ij} & \sum_{i=22}^{26}\sum_{j=22}^{26} C_{ij} & \sum_{i=22}^{26}\sum_{j=27}^{32} C_{ij} \\ \sum_{i=27}^{32}\sum_{j=1}^{14} C_{ij} & \sum_{i=27}^{32}\sum_{j=15}^{21} C_{ij} & \sum_{i=27}^{32}\sum_{j=22}^{26} C_{ij} & \sum_{i=27}^{32}\sum_{j=27}^{32} C_{ij} \end{bmatrix},$$

where N_1, N_2, N_3, and N_4 denote the number of wires in each group, and the indices of wires in G1 are from 1 to 14, in G2 from 15 to 21, in G3 from 22 to 26, and in G4 from 27 to 32.

Geometry for the equivalent harness is required for full-wave simulation of the radiated emissions prediction. The height above the return plane of the four wires in the reduced harness was set equal to the average height of the wires within each group. That is:

$$\begin{aligned} \bar{h_1} &= \frac{1}{14}\sum_{i=1}^{14} h_i, \bar{h_2} = \frac{1}{7}\sum_{j=15}^{21} h_j, \\ \bar{h_3} &= \frac{1}{5}\sum_{m=22}^{26} h_m, \bar{h_n} = \frac{1}{6}\sum_{n=27}^{32} h_n, \end{aligned} \tag{6}$$

where h_i, h_j, h_m, h_n are the heights of i^{th}, j^{th}, m^{th} and n^{th}cables, respectively.

The radius of each equivalent reduced conductor can be set to realize the target self-inductance of the reduced harness as [6]:

$$r_k = 2\bar{h}_k \cdot exp(-\frac{2\pi}{\mu_0} L_{kk}^{reduced}), \tag{7}$$

where k =1, 2, 3 or 4, denoting group 1, group 2, group 3 or group 4.

The distance between the conductors is set to realize the mutual inductances in the $\bar{\bar{L}}_{reduced}$ between each pair of equivalent reduced conductors as [6]:

$$d_{i,j} = \sqrt{\frac{4\bar{h}_i\bar{h}_j}{exp(\frac{4\pi}{\mu_0} L_{i,j}^{reduced}) - 1}} \tag{8}$$

where i, j =1, 2, 3 or 4, related to G1, G2, G3 and G4; and $d_{i,j}$ means the distance between equivalent wire i and wire j.

The geometry for the equivalent harness bundle studied here is shown in Figure 18).

6. ANTENNA MODEL

The radiated emissions related to the ECU and harness in the tests were found by modeling both the antenna, the ECU and harness setup.

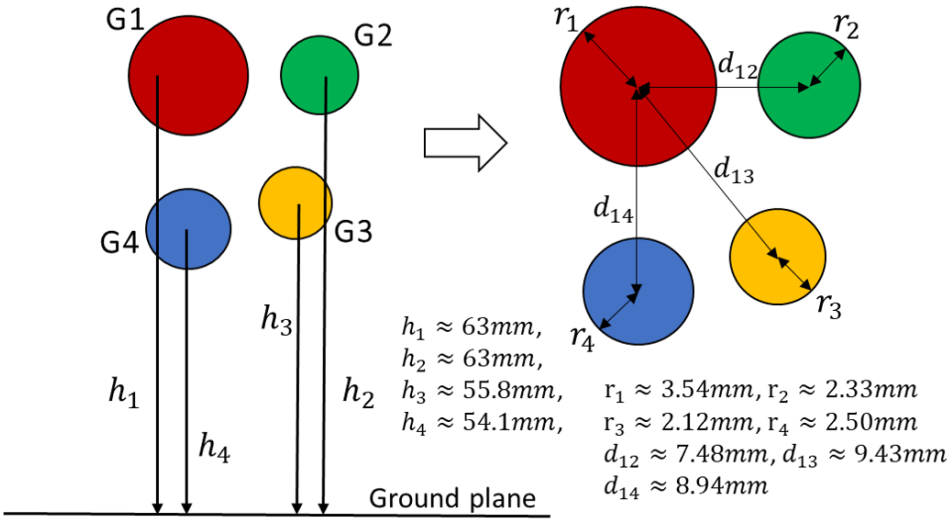

Figure 18. The approximated cross-section of the cable harness.

The antenna used in this test was a VHBB 9124 4:1 BALUN, provided from SCHWARTZBECK MESS. The geometry of the antenna was reproduced in the full-wave simulation environment with CST Microwave Studio as shown in Figure 19).

Considering the 4:1 BALUN of the antenna, the discrete port with a 200 Ω characteristic impedance was assigned at the antenna port location. The round rods of the antenna was modelled as rectangular bars to reduce the total mesh count with little expected impact on the simulated electrical performance of the antenna.

The validity of the full-wave simulation was determined by comparing the properties of antenna model with the values in the datasheet for 3 measures: the voltage standing wave ratio (VSWR), the isotropic gain, and the antenna factor (AF).

The comparison between simulation results of antenna model and those values in the datasheet is shown for the gain and antenna factor in Figure 19). The discrepancy between simulation model and values in datasheet are within 3 dB from 20 to 300 MHz.

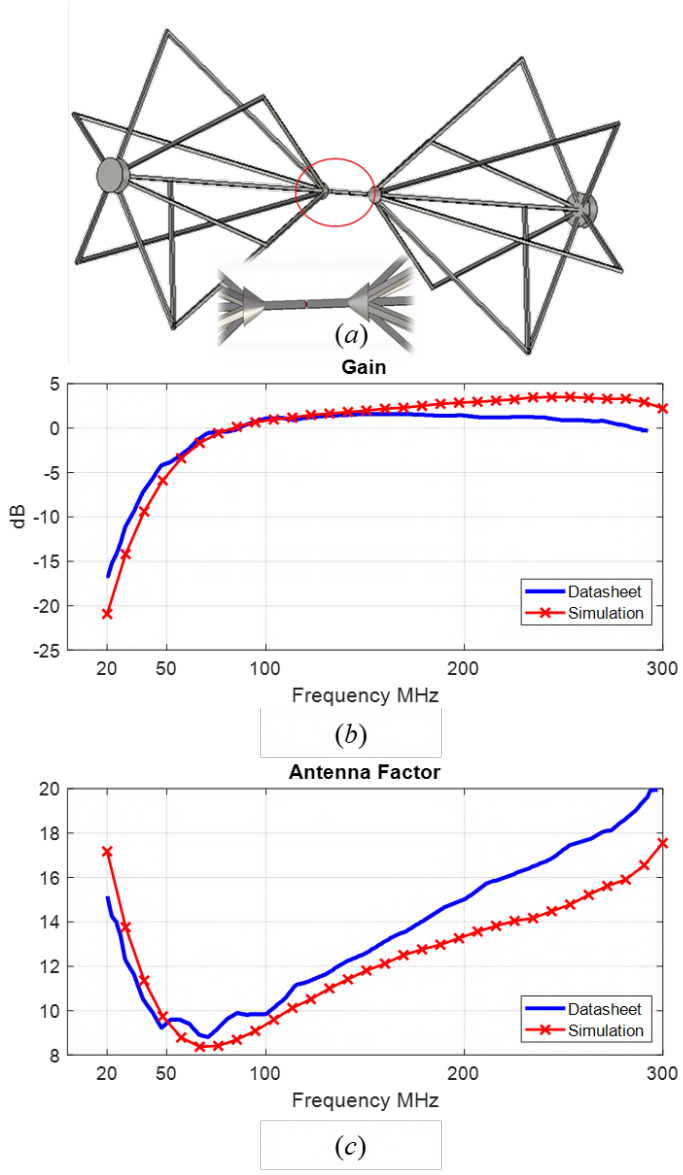

Figure 19. (a) The antenna model. A 200 Ω port was assigned between the two conical parts. (b) The isotropic gain. (c) The antenna factor.

7. EMI TEST SETUP MODEL

A 3D model was built in CST to reproduce the test setup in Figure 1. The antenna model was required since the measurement was not in the far-field over the frequency range of interest (20-300 MHz). The setup includes the receiving biconical antenna, the ground plane, the simplified cable harness, ECU, LISN, and load pads, as shown in Figure 20.

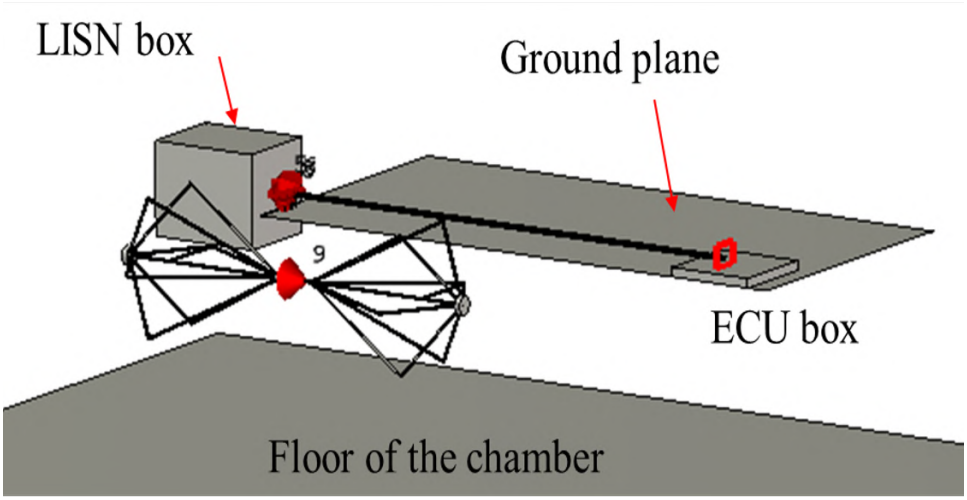

Figure 20. The setup used to measure radiated emissions from the ECU (horizontal polarized antenna).

The ECU and LISN were modelled as rectangular blocks. The LISN and ECU chassis were electrically connected to the ground plane by copper tape, and this connection was mimicked in the simulation model. The wire representing the group G1 in the equivalent harness was connected to the LISN via a 50-Ω port. Other three 50-Ω ports at load side were connected to load pads. The load pads were metal ground of PCB loads, shown in Figure 21. At source side, to keep the good transmission of TEM wave, there was a waveguide port with 4 pins used to connect the equivalent harness to the ECU, shown in Figure 22. As mentioned in antenna model, a 200-Ω discrete port was set at the antenna port. Results were found for both vertical or horizontal polarization. The bottom simulation boundary was set as perfect electrical conductor (PEC), and the other five boundaries were set as perfect matched layer (PML) to mimic the semi-anechoic chamber conditions.

Full-wave simulations were performed with the antenna in a vertical and horizontal polarization to find the S-parameters relating the nine ports with one another. These S-parameters were used in a SPICE model as shown in Figure 23 to combine the full-wave

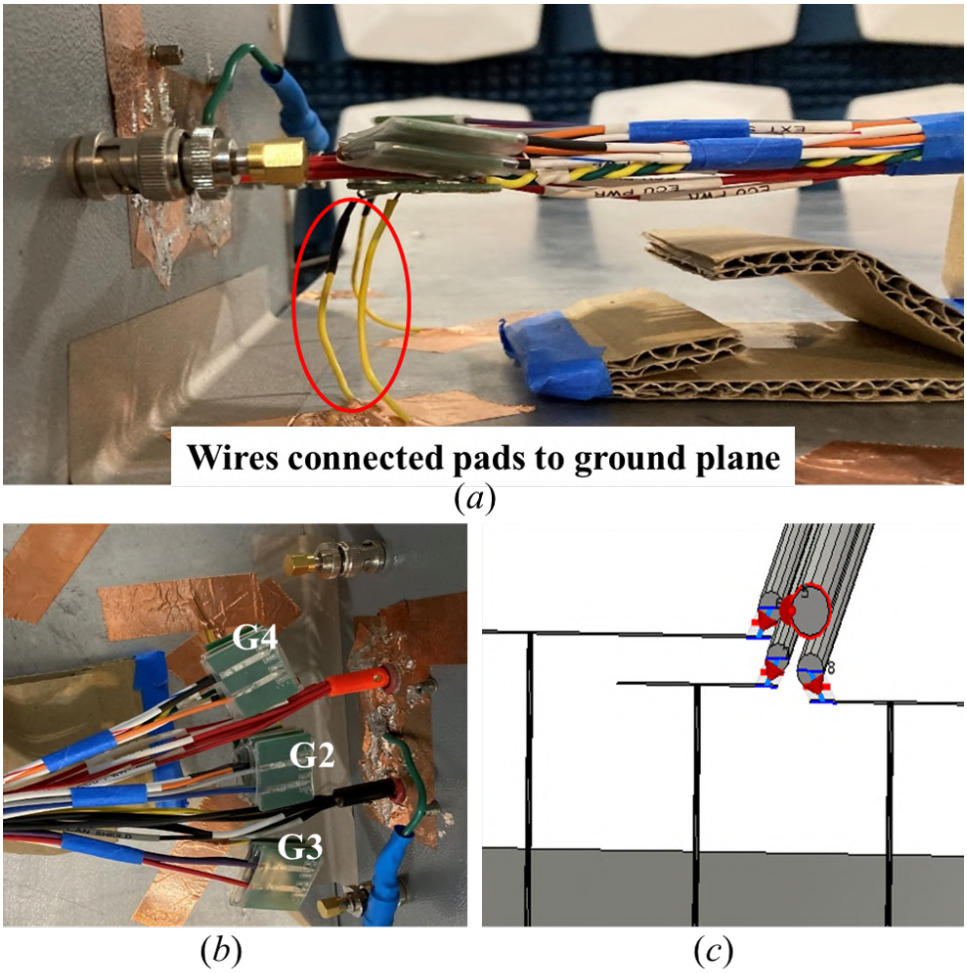

Figure 21. (a) The side view of PCB loads. (b) The top view of loads. (c) The load model in CST with pads.

radiated emissions model with the SPICE models of the ECU sources and loads. The antenna is represented by a 200 Ω resistor in this circuit. The simulated radiated power is then found from the power received by this 200 Ω resistor as:

$$EMI = dBm\left(\frac{V_{ant}^2}{2 \times 200\Omega}\right) \tag{9}$$

where V_{ant} is the voltage on the 200 Ω antenna port.

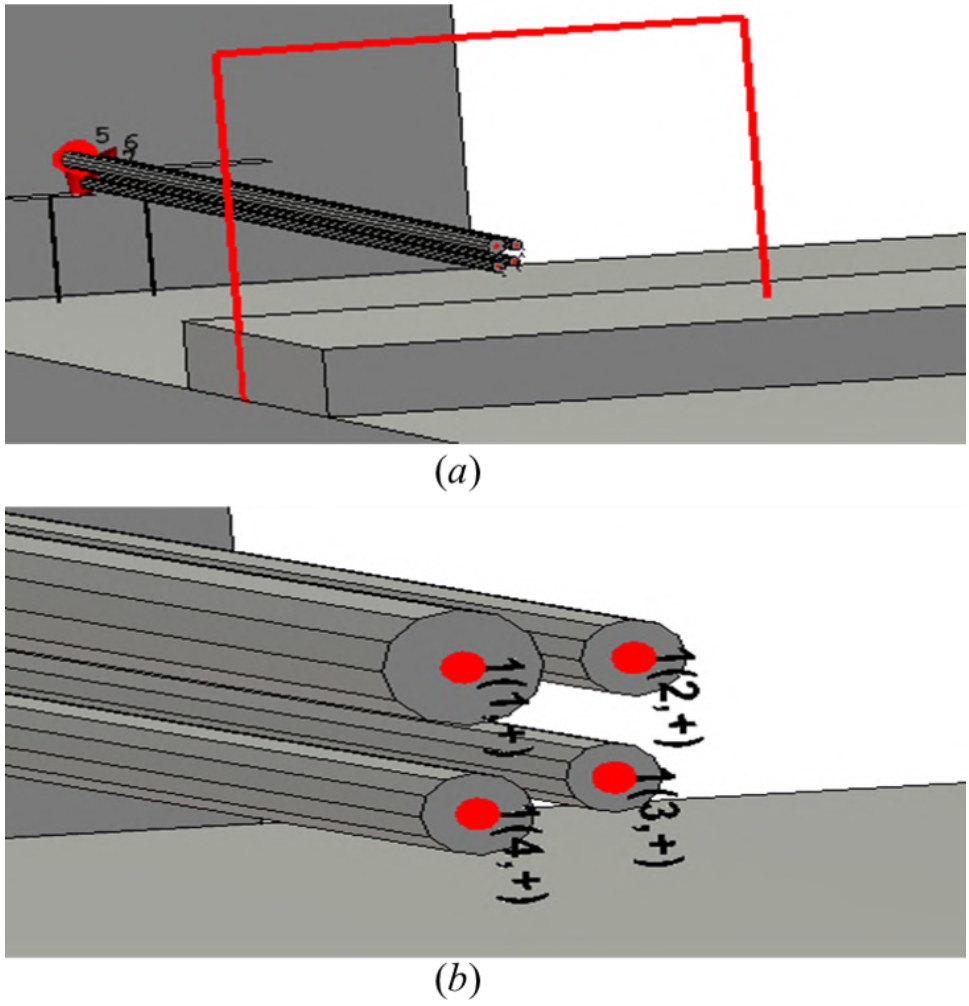

Figure 22. (a) Waveguid port connections at the ECU side. (b) A closer view of multipin port.

8. VALIDATION AND CONCLUSIONS

To adequately account for the amplifier and instrument noise seen in measurements, the noise floor was added to the predictions found in (9), to give a "noisy" estimate of radiated emissions:

$$EMI = dBm\left(\frac{V_{ant}^2}{2 \times 200\Omega} \cdot Gain + Noise\right) \tag{10}$$

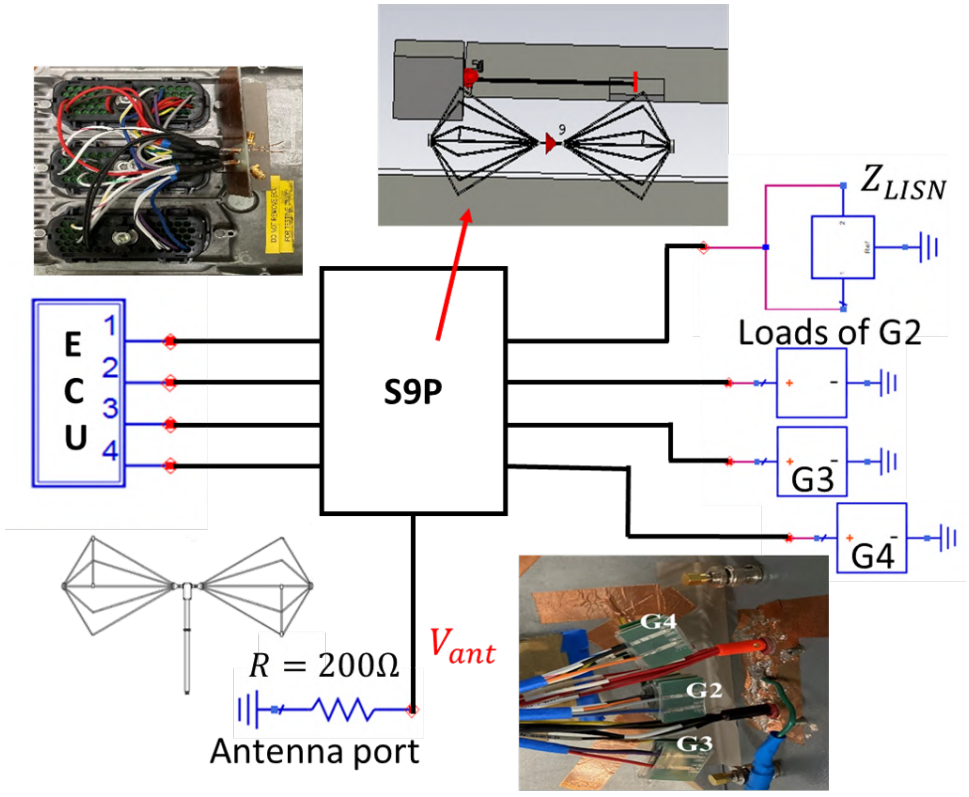

Figure 23. The circuit simulation combining all components to predict the radiated emission.

where Gain is the amplifier gain and noise is the noise floor of the spectrum analyzer when using a 100 kHz RBW with the amplifier.

The comparison results of predicted and measured radiated emissions are shown in Figure 24 for both vertical and horizontal antenna polarizations. Compared with measured radiated emission levels, the predicted radiated emissions are within around 3 dB.

The results shown in Figure 24 are for the simplest case, where the harness is driven at a fixed height across a continuous return plane. The harness length is very short, around 1 m, so only one major peak can be observed on both vertical and horizontal polarizations, and therefore, for this simplest case, the major peaks in the measurements are also captured well.

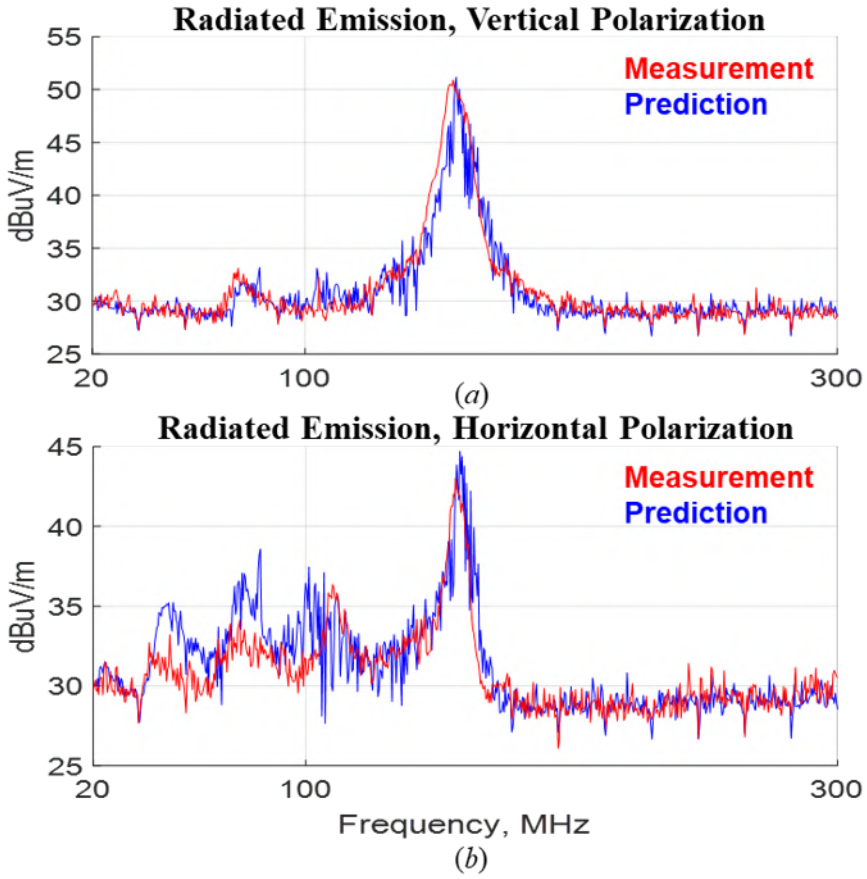

Figure 24. Comparison of measured and predicted radiated emissions for a 1 m long harness above a metal return plane. (a) Vertical polarization. (b) Horizontal polarization.

To test the limits of this proposed method, a longer harness which is 161 cm long. As harness length gets longer, more peaks of radiated emissions can be measured. The comparison results are shown in Figure 25.

In general, the simulation and measurement results still have a good correlation and the discrepancy is within 3 dB. On vertical polarization, the major peak levels in the predicted radiated emission results match the measured levels very well, within 1 dB. On horizontal polarization, though the major peak levels captured in predicted radiated emission results are within 3 dB, there is a resonance off problem for the peak at around 160 MHz.

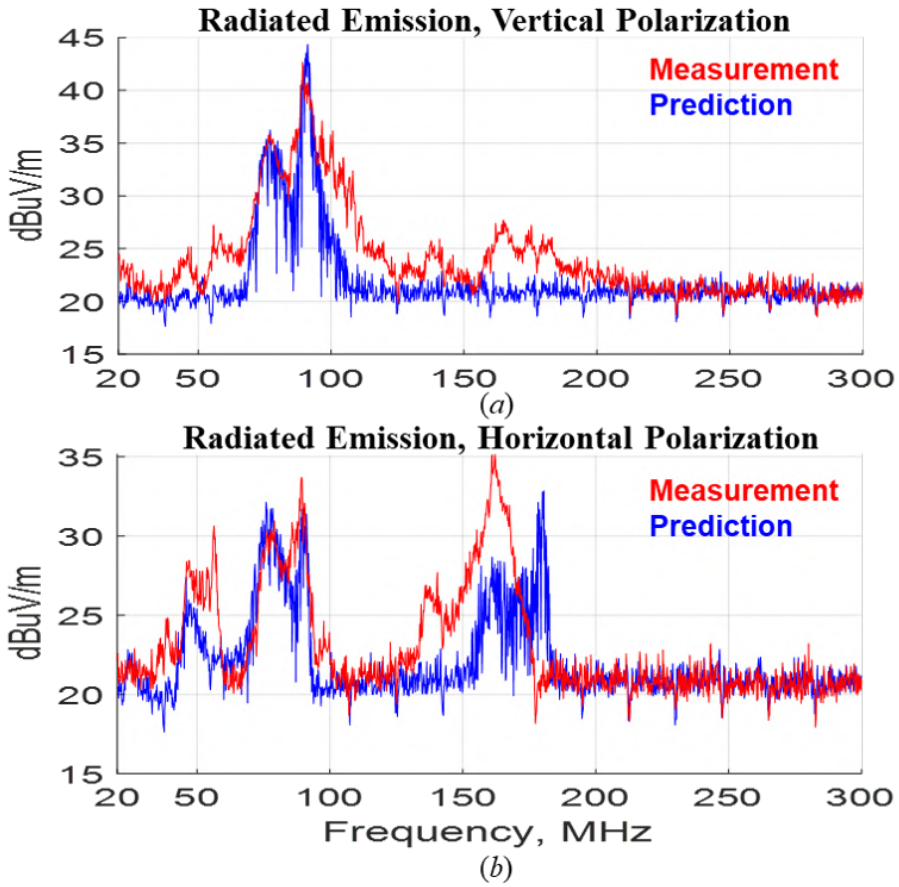

Figure 25. Comparison of measured and predicted radiated emissions for a 161 cm long harness above a metal return plane. (a) Vertical polarization. (b) Horizontal polarization.

Usually, in a real vehicle, the distance from the harness to the vehicle chassis will often change along the length of the harness. In order to make the test setup more in line with the actual situation, such a scenario is shown in Figure 26.

The starting location of the arc is 51 cm away from the LISN; the highest point of the arc is 32 cm higher than the ground plane, and the arc width is 31 cm. Simulated and measured emissions compared results are shown in Figure 27. The comparison results show good consistency in trend, in terms of the correct resonance frequency of major peaks, and peak emissions continue to be captured within 6 dB. Comparing the results on vertical and

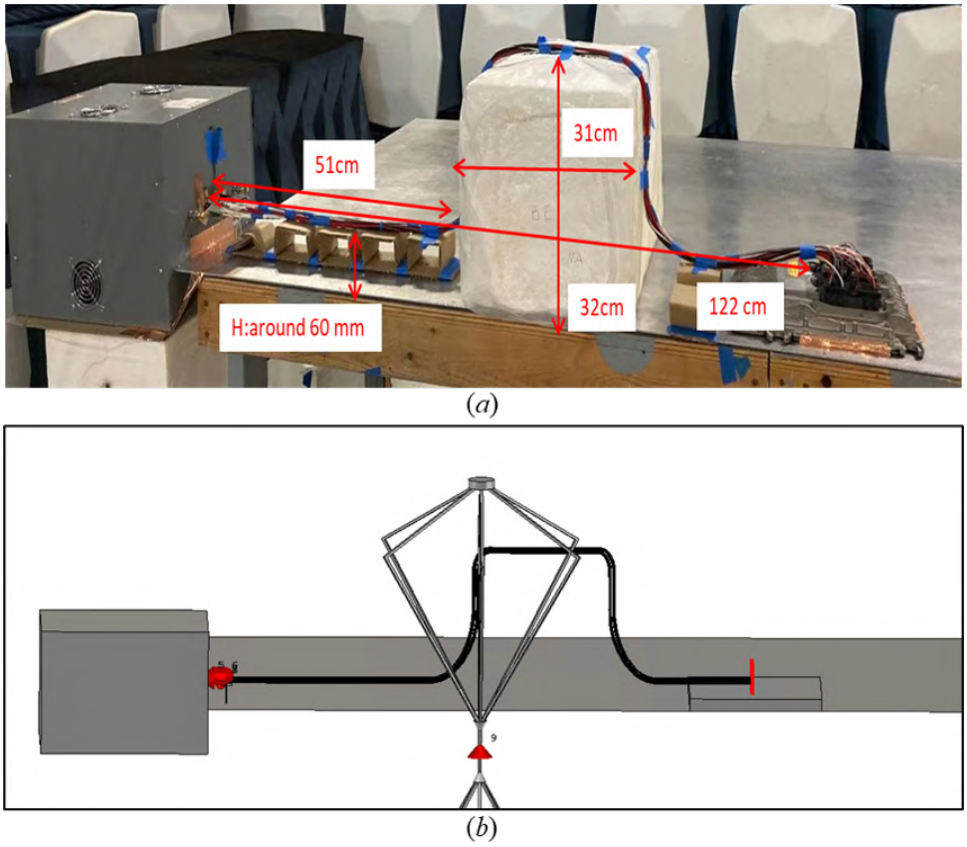

Figure 26. Bend harness case. (a) Test setup. (b) Full-wave model of the test setup in CST.

horizontal polarizations, there shows a better correlation on horizontal antenna polarization and the captured peak emissions are within 3 dB. However, on vertical polarization, the discrepancy gets larger, only within 6 dB.

The more practical scenario in a real vehicle is that there are many branches at the extremity of the cable harness bundle to connect different sensors and loads at different locations. Hence, the scenario of branch case at the far end location away from the ECU source is built, and the loads of group 3 are moved to a location far from the harness bundle to form a branch, shown in Figure 28. The length of the branch is about 27 cm, accounting for 16.7% of the total 161 cm harness length.

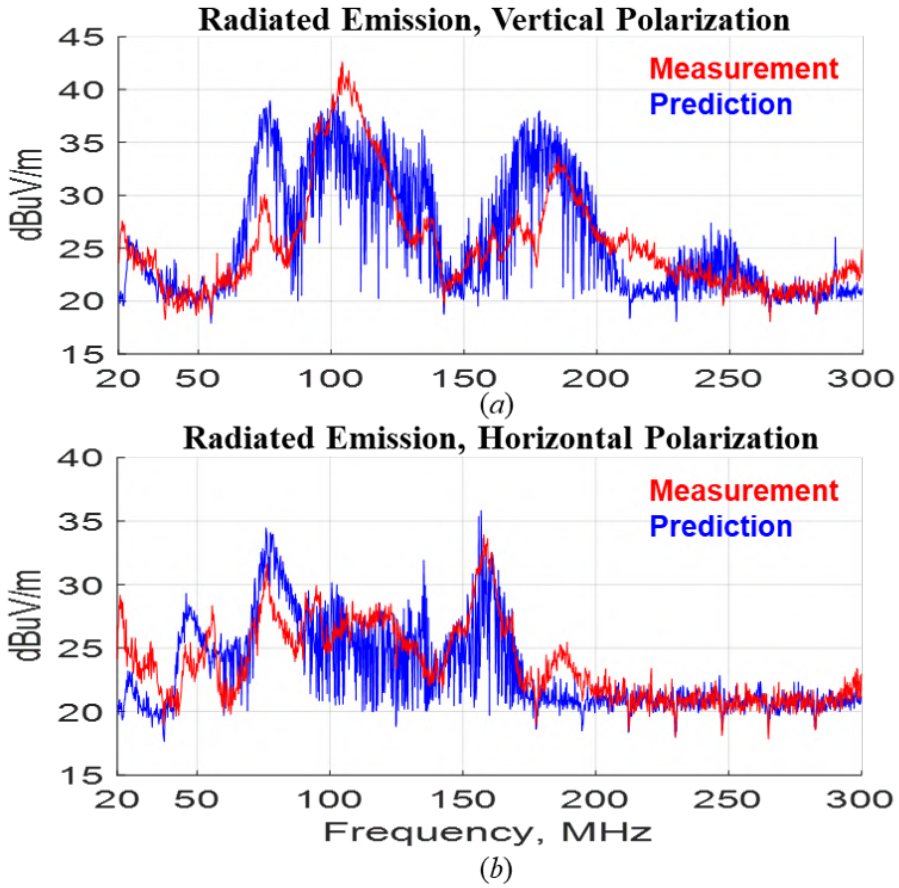

Figure 27. Comparison of measured and predicted radiated emissions for bend harness case. (a) Vertical polarization. (b) Horizontal polarization.

Figure 29 shows the comparison results of measured and predicted radiated emissions for branch harness case. Obviously, the peak emissions continue to be captured within 6 dB. Focusing on vertical polarization, the major peak emission level of predicted results has strong consistency with measurement data, within 3 dB. For horizontal polarization results, a larger discrepancy is observed in the peak around 160 MHz, within 6 dB.

In this paper, a procedure is proposed to predict the system-level radiated emissions from the harness connected to an electronic component source. The prediction of system-level radiated emissions test could be broken down into five different blocks and model these blocks separately. For each block, the procedure of characterization and model

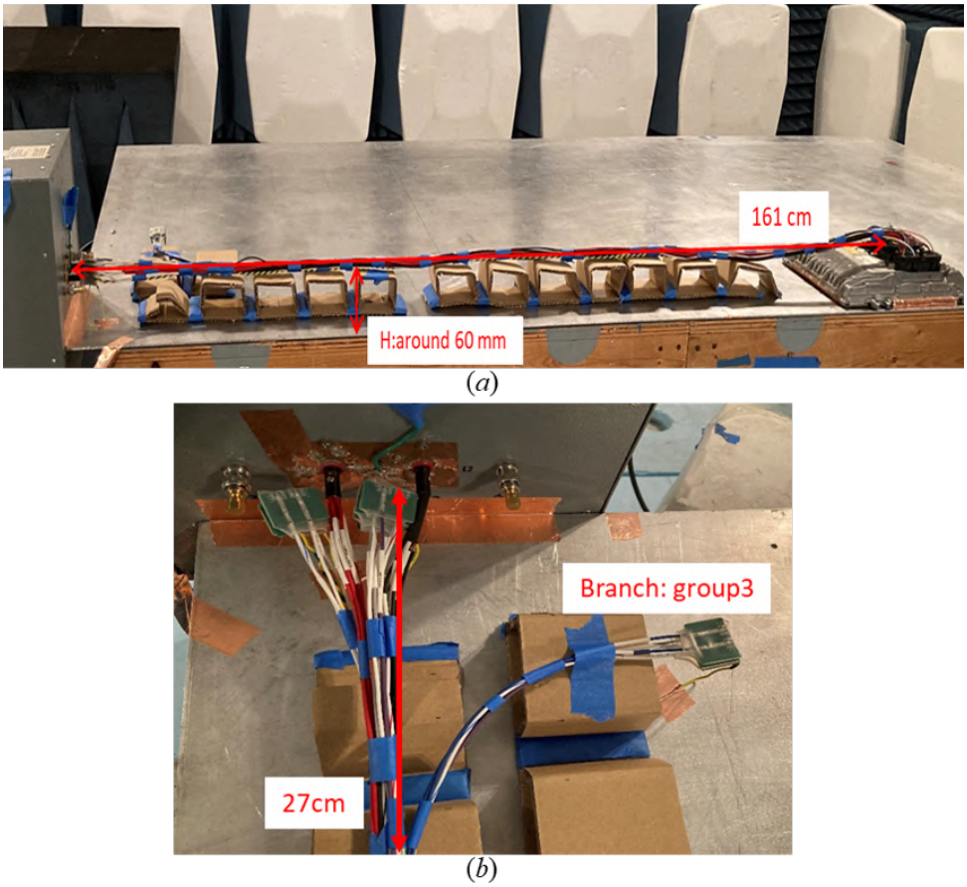

Figure 28. Branch harness case. (a) Test setup. (b) A closer view of the branch.

uses only component level tests. For common-mode source part, a more universal source characterization method is developed to extract the equivalent source information from engine control units with different shapes, based on the vertical plane cut along the harness. The very pivotal part is the harness reduction, and with the cable harness simplified from 32-wire to 4-wire equivalent multiconductor transmission line while maintaining the per-unit-length L and C matrices of the harness, the complexity of building the harness model and 3D full-wave simulation is reduced dramatically. The overall system-level radiated emission test setup is simulated in a full-wave solver, which yields an S-parameter matrix. Eventually, all the characterized blocks are connected to the pivotal s9p file exported from the CST simulation in a SPICE model. The proposed procedure is tested under bend harness

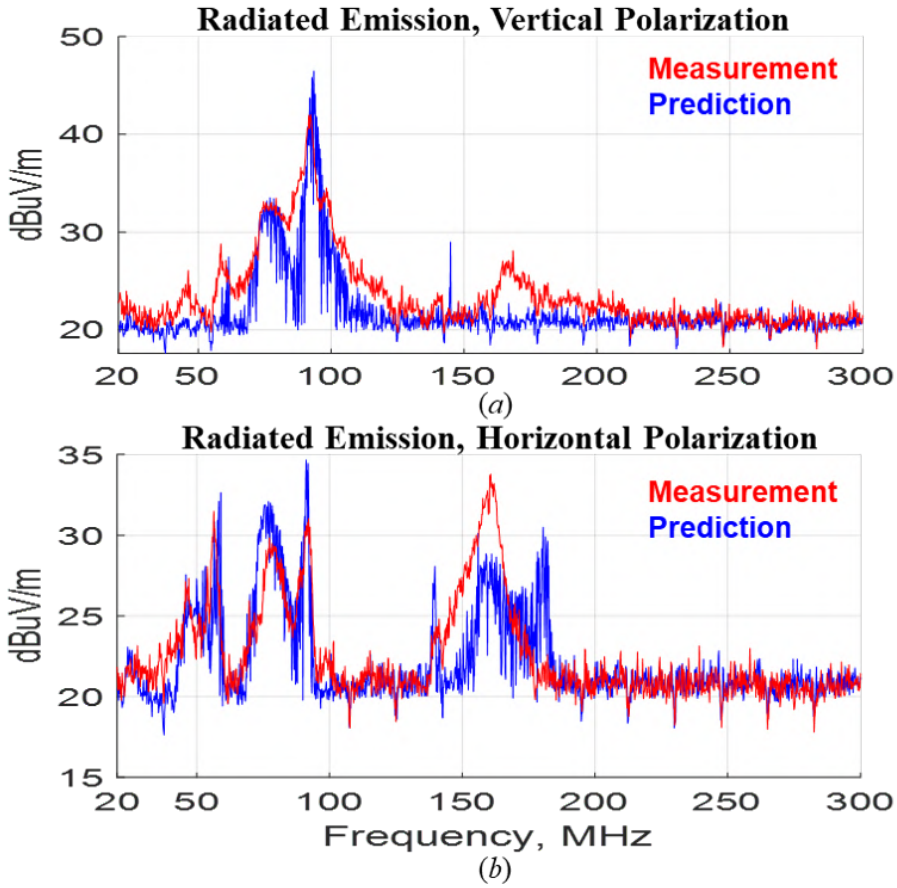

Figure 29. Comparison of measured and predicted radiated emissions for branch harness case. (a) Vertical polarization. (b) Horizontal polarization.

case and branch harness case. For both cases, the prediction results show the good accuracy in predicting the peak levels in the radiated emissions, within 6 dB. Therefore, the proposed procedure is a reliable approach in predicting the EMI performance of system-level tests in the initial design stage. The component-level measurements can be conducted separately and simultaneously. The design guideline and margin for EMI compliance can be updated by conducting the procedure and allow for inexpensive solutions for emissions issues.

In future work, the impact of dielectric layer should be discussed. The resonance off problem for the peak at around 160 MHz observed in horizontal polarization for branch harness case is related to the dielectric layer around the wires, which will influence the per-unit-length C matrix.

ACKNOWLEDGEMENTS

This paper is based upon work supported partially by the National Science Foundation under Grant No. HP-1916535.

REFERENCES

[1] R. Zamir, V. Bar-Natan, and E. Recht. System level emc - from theory to practice. In *2005 International Symposium on Electromagnetic Compatibility, 2005. EMC 2005.*, volume 3, pages 741–743 Vol. 3, 2005. doi: 10.1109/ISEMC.2005.1513622.

[2] Tamar Makharashvili, Sameer Arun Walunj, Ruijie He, Brian Booth, Kerry Martin, Chulsoon Hwang, and Daryl G. Beetner. Prediction of common mode current in cable harnesses. In *2018 IEEE International Symposium on Electromagnetic Compatibility and 2018 IEEE Asia-Pacific Symposium on Electromagnetic Compatibility (EMC/APEMC)*, pages 321–326, 2018. doi: 10.1109/ISEMC.2018.8393790.

[3] Sameer Walunj, Fuwei Ma, Tamar Makharashvili, Ruijie He, Chulsoon Hwang, Daryl Beetner, Brian Booth, and Kerry Martin. Experimental characterization of the common-mode current sources in a cable harness. In *2019 IEEE International Symposium on Electromagnetic Compatibility, Signal Power Integrity (EMC+SIPI)*, pages 292–297, 2019. doi: 10.1109/ISEMC.2019.8825258.

[4] Chinchi Chen. Predicting vehicle-level radiated emi emissions using module-level conducted emis and harness radiation efficiencies. In *2001 IEEE EMC International Symposium. Symposium Record. International Symposium on Electromagnetic Compatibility (Cat. No.01CH37161)*, volume 2, pages 1146–1151 vol.2, 2001. doi: 10.1109/ISEMC.2001.950586.

[5] Wissem Yahyaoui, Lionel Pichon, and Fabrice Duval. A 3d peec method for the prediction of radiated fields from automotive cables. *IEEE Transactions on Magnetics*, 46(8):3053–3056, 2010. doi: 10.1109/TMAG.2010.2043823.

[6] Guillaume Andrieu, Lamine KonÉ, FrÉdÉric Bocquet, Bernard DÉmoulin, and Jean-Philippe Parmantier. Multiconductor reduction technique for modeling common-mode currents on cable bundles at high frequency for automotive applications. *IEEE Transactions on Electromagnetic Compatibility*, 50(1):175–184, 2008. doi: 10.1109/TEMC.2007.911914.

[7] Zhuo Li, Zhi Jiang Shao, Ji Ding, Zhen Yi Niu, and Chang Qing Gu. Extension of the "equivalent cable bundle method" for modeling crosstalk of complex cable bundles. *IEEE Transactions on Electromagnetic Compatibility*, 53(4):1040–1049, 2011. doi: 10.1109/TEMC.2011.2146258.

[8] V. S. Reddy, Peter Kralicek, and Jan Hansen. A novel segmentation approach for modeling of radiated emission and immunity test setups. *IEEE Transactions on Electromagnetic Compatibility*, 59(6):1781–1790, 2017. doi: 10.1109/TEMC.2017.2699480.

[9] Sameer Walunj, Tamar Makharashvili, Chulsoon Hwang, Daryl Beetner, Brian Booth, and Kerry Martin. Direct measurement and representation of common-mode sources in cable harnesses. In *2020 IEEE International Symposium on Electromagnetic Compatibility Signal/Power Integrity (EMCSI)*, pages 118–120, 2020. doi: 10.1109/EMCSI38923.2020.9191589.

[10] Heinz Rebholz and Stefan Tenbohlen. A fast radiated emission model for arbitrary cable harness configurations based on measurements and simulations. In *2008 IEEE International Symposium on Electromagnetic Compatibility*, pages 1–5, 2008. doi: 10.1109/ISEMC.2008.4652041.

SECTION

2. SUMMARY AND CONCLUSIONS

In this thesis, a procedure is proposed to predict the system-level radiated emissions from the harness connected to an electronic component source and this procedure uses only component level tests. The prediction of system-level radiated emissions test could be broken down into five different blocks and model these blocks separately. The outline for predicting radiated emissions procedure based on component level tests is shown in Figure 2.1. The common-mode source inside ECU will be characterized first as step I., then the step II., III., and step IV. can be conducted separately or at the same time.

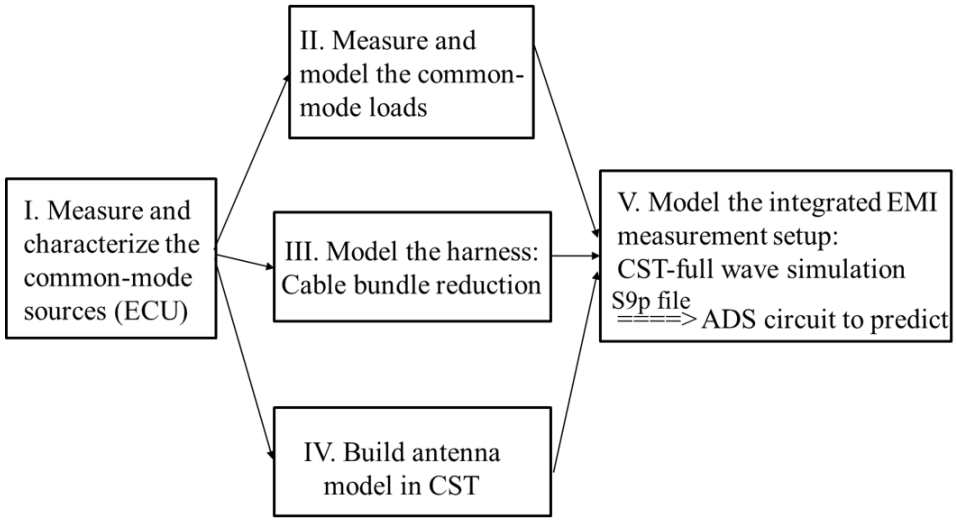

Figure 2.1. The outline for prediction procedure.

For common-mode source part, a more universal source characterization method is developed to extract the equivalent source information from engine control units (ECUs) with different shapes, based on the vertical plane cut along the harness.

The proposed procedure is tested under variety harness configurations. Among those cases, the prediction results show the good accuracy in predicting the peak levels in the radiated emissions. Predicted emissions predict measured levels of emissions within 6 dB and the results are within the target accuracy for project purpose.

REFERENCES

[1] Guillaume Andrieu, Lamine KonÉ, FrÉdÉric Bocquet, Bernard DÉmoulin, and Jean-Philippe Parmantier. Multiconductor reduction technique for modeling common-mode currents on cable bundles at high frequency for automotive applications. *IEEE Transactions on Electromagnetic Compatibility*, 50(1):175–184, 2008. doi: 10.1109/TEMC.2007.911914.

[2] R. Zamir, V. Bar-Natan, and E. Recht. System level emc - from theory to practice. In *2005 International Symposium on Electromagnetic Compatibility, 2005. EMC 2005.*, volume 3, pages 741–743 Vol. 3, 2005. doi: 10.1109/ISEMC.2005.1513622.

[3] Tamar Makharashvili, Sameer Arun Walunj, Ruijie He, Brian Booth, Kerry Martin, Chulsoon Hwang, and Daryl G. Beetner. Prediction of common mode current in cable harnesses. In *2018 IEEE International Symposium on Electromagnetic Compatibility and 2018 IEEE Asia-Pacific Symposium on Electromagnetic Compatibility (EMC/APEMC)*, pages 321–326, 2018. doi: 10.1109/ISEMC.2018.8393790.

[4] Sameer Walunj, Fuwei Ma, Tamar Makharashvili, Ruijie He, Chulsoon Hwang, Daryl Beetner, Brian Booth, and Kerry Martin. Experimental characterization of the common-mode current sources in a cable harness. In *2019 IEEE International Symposium on Electromagnetic Compatibility, Signal Power Integrity (EMC+SIPI)*, pages 292–297, 2019. doi: 10.1109/ISEMC.2019.8825258.

[5] Chinchi Chen. Predicting vehicle-level radiated emi emissions using module-level conducted emis and harness radiation efficiencies. In *2001 IEEE EMC International Symposium. Symposium Record. International Symposium on Electromagnetic Compatibility (Cat. No.01CH37161)*, volume 2, pages 1146–1151 vol.2, 2001. doi: 10.1109/ISEMC.2001.950586.

[6] Wissem Yahyaoui, Lionel Pichon, and Fabrice Duval. A 3d peec method for the prediction of radiated fields from automotive cables. *IEEE Transactions on Magnetics*, 46(8):3053–3056, 2010. doi: 10.1109/TMAG.2010.2043823.

[7] Zhuo Li, Zhi Jiang Shao, Ji Ding, Zhen Yi Niu, and Chang Qing Gu. Extension of the "equivalent cable bundle method" for modeling crosstalk of complex cable bundles. *IEEE Transactions on Electromagnetic Compatibility*, 53(4):1040–1049, 2011. doi: 10.1109/TEMC.2011.2146258.

[8] V. S. Reddy, Peter Kralicek, and Jan Hansen. A novel segmentation approach for modeling of radiated emission and immunity test setups. *IEEE Transactions on Electromagnetic Compatibility*, 59(6):1781–1790, 2017. doi: 10.1109/TEMC.2017.2699480.

[9] Sameer Walunj, Tamar Makharashvili, Chulsoon Hwang, Daryl Beetner, Brian Booth, and Kerry Martin. Direct measurement and representation of common-mode sources in cable harnesses. In *2020 IEEE International Symposium on Electromagnetic Compatibility Signal/Power Integrity (EMCSI)*, pages 118–120, 2020. doi: 10.1109/EMCSI38923.2020.9191589.

[10] Heinz Rebholz and Stefan Tenbohlen. A fast radiated emission model for arbitrary cable harness configurations based on measurements and simulations. In *2008 IEEE International Symposium on Electromagnetic Compatibility*, pages 1–5, 2008. doi: 10.1109/ISEMC.2008.4652041.

VITA

Fuwei Ma was born in Chongqing, China, in 1997. He received the B.E. degree in electrical engineering from the Huazhong University of Science and Technology, Wuhan, China, in 2015.

He received the M.S. degree in Electrical Engineering from the Missouri University of Science and Technology, Rolla, MO, USA, in May 2022. He joined the Electromagnetic Compatibility Laboratory as graduate research assistant from 2019 to 2022.

His research interests included electromagnetic compatibility, electromagnetic immunity, and signal integrity in high-speed digital systems.